INTERNATIONAL JOURNAL FOR NUMERICAL METHODS IN FLUIDS
*Int. J. Numer. Meth. Fluids* 2002; **40**:1561–1570 (DOI: 10.1002/fld.412)

# The *hp* mortar domain decomposition method for problems in fluid mechanics

Lawrence K. Chilton[1] and Padmanabhan Seshaiyer[2,*,†]

[1] *Department of Mathematics and Statistics, Air Force Institute of Technology, WPAFB, OH 45433, U.S.A.*
[2] *Department of Mathematics and Statistics, Texas Tech University, Lubbock, TX 79409-1042, U.S.A.*

## SUMMARY

We consider the incompressible Stokes equations in primal velocity–pressure variables and present the mortar finite element formulation for this problem. The local approximation within each subdomain is designed using divergence stable *hp*-mixed finite elements. The velocity is computed in a mortared space while the pressure is not subjected to any constraints across the interfaces. Our computational results show that the mortar finite element method for the Stokes problem satisfies similar rates of convergence as the conforming finite element method, in the presence of various *h*, *p* and *hp* discretizations (including the case of exponential *hp* convergence over geometric meshes). We also present the numerical results for the Lagrange multiplier when the method is implemented as a mixed method. Copyright © 2002 John Wiley & Sons, Ltd.

KEY WORDS: *hp*-version; mortar elements; finite elements; non-conforming

## 1. INTRODUCTION

Over the last few years, there has been a significant development in non-overlapping domain decomposition techniques for rigourously coupling different physical processes, that are modelled independently over different subdomains. During this coupling (*assembly*) however, it is often too cumbersome, or even infeasible to co-ordinate the individually modelled sub-components so that they conform at the interfaces. Using conforming techniques, one must perform transition modelling to co-ordinate the meshes, which can become quite complex, tedious and expensive in such cases because the finite element nodes of each component at the common interface are not, in general, coincident. This motivates the necessity for non-conforming methods at the sub-domain level.

The mortar finite element method introduced by Bernardi *et al.* in Reference [1] is an example of a non-conforming technique which can be used to de-compose and re-compose a domain into subdomains without requiring compatibility between the meshes on the separate components. This technique can help achieve *efficient* solutions for problems involving

* Correspondence to: P. Seshaiyer, Department of Mathematics and Statistics, Texas Tech University, Lubbock, TX 79409-1042, U.S.A.
† E-mail: padhu@math.ttu.edu

*Received 1 November 2001*
*Revised 12 June 2002*

non-matching grids in fluid mechanics. For instance, it allows the selective use of locally structured grids in different subdomains which is particularly helpful in the presence of boundary layers that often arise in computational fluid dynamics. Moreover it also leads to fast local solvers.

Although, one can achieve efficient solutions via the traditional mortar finite element method, it is also important to simultaneously guarantee that these numerical solutions are also *accurate*. One way to achieve this is to employ the mortar finite element formulation in conjunction with *higher-order* elements. The use of such high order elements can be realized in terms of the *hp*-version of the finite element method, where both mesh refinement (*h*-version) and degree enhancement ($p$-version) are combined to increase accuracy. This is particularly helpful for solutions to boundary value problems of incompressible fluid flow in non-smooth domains that exhibit well-known corner singularities (even if the prescribed data are piecewise analytic) and other phenomena such as locking. Note that the *hp*-version can, with proper mesh-degree selection, lead to *exponential* convergence rates (see References [2–4]). The correct design of elements and underlying method is therefore crucial, and is the issue we address in this paper.

The *hp*-version of the mortar finite element method was first developed for the Poisson problem by Seshaiyer and Suri in Reference [5]. The stability and convergence of this technique in the *hp* context was analyzed and tested computationally (see References [6–9]). The mathematical theory of mortaring for the incompressible Stokes equations has been presented for the *h*-version by Ben Belgacem in Reference [10] and by Achdou *et al.* in Reference [11]. It was also extended to spectral elements by Ben Belgacem *et al.* in Reference [12] and for the *hp*-version by Ben Belgacem *et al.* in Reference [13]. Some related applications to fluids can be found in References [14–16].

The purpose of this paper is to computationally validate the convergence behaviour for the *hp* mortar finite element formulation for the Stokes boundary value problem for viscous incompressible fluid flow. In particular, we recover exponential convergence for these techniques in the presence of highly non-quasiuniform geometric meshes. Our numerical results for $h$, $p$ and *hp* mortar finite element methods show that these methods behave as well as conforming finite element methods both in the presence of non-conformity in the mesh and polynomial degree. Our computations also indicate that stress extraction can be accurately performed even along the interfaces when mortar methods are used for the Stokes problem.

## 2. WEAK FORMULATION OF STOKES PROBLEM AND ITS DISCRETIZATION

Consider the Stokes boundary value cproblem for viscous incompressible fluid flow over a domain $\Omega \subset \mathbb{R}^2$ (with boundary $\partial\Omega$): Find a velocity field $\mathbf{u} = (u_1, u_2)$ and a pressure $p$ such that,

$$-\mu\Delta\mathbf{u} + \nabla p = \mathbf{f} \quad \text{in } \Omega, \qquad \nabla \cdot \mathbf{u} = 0 \text{ in } \Omega, \qquad \mathbf{u} = 0 \text{ on } \partial\Omega \tag{1}$$

Here, $\mu > 0$ is the kinematic viscosity which is related to the Reynolds number of the flow. The right hand side $\mathbf{f} = (f_1, f_2)$ is a given body force per unit mass.

Define $L_0^2(\Omega)$ to be the space of real-valued square-integrable functions with vanishing mean value. Let $H_0^1(\Omega) = \{u \in H^1(\Omega) \mid u = 0 \text{ on } \partial\Omega\}$ and denote $\mathbf{H}_0^1(\Omega) = H_0^1(\Omega) \times H_0^1(\Omega)$. Here we have used standard Sobolev space notation. Both spaces $L_0^2(\Omega)$ and $\mathbf{H}_0^1(\Omega)$ are provided with the norms and seminorms in the usual sense and $(.,.)$ is the usual $L^2(\Omega)$ inner product. We can rewrite (1) as a weak formulation: Find a velocity field $\mathbf{u}\in\mathbf{H}_0^1(\Omega)$ and a pressure $p\in L_0^2(\Omega)$ such that,

$$\mu(\nabla\mathbf{u},\nabla\mathbf{v})-(\nabla\cdot\mathbf{v},p)=(\mathbf{f},\mathbf{v}) \quad \text{and} \quad (\nabla\cdot\mathbf{u},q)=0 \tag{2}$$

for all $(\mathbf{v},q)\in\mathbf{H}_0^1(\Omega)\times L_0^2(\Omega)$. Let us denote $b(\mathbf{v},q)=-(\nabla\cdot\mathbf{v},q)$. For $\mathbf{f}\in\mathbf{L}^2(\Omega)=L^2(\Omega)\times L^2(\Omega)$, one can show using Brezzi's saddle-point theory [17] that the problem (2) is well posed and has a unique solution $(\mathbf{u},p)\in\mathbf{H}_0^1(\Omega)\times L_0^2(\Omega)$. This follows from the following continuous *inf–sup* condition:

$$\inf_{q\in L_0^2(\Omega)}\sup_{\mathbf{v}\in\mathbf{H}_0^1(\Omega)}\frac{b(\mathbf{v},q)}{\|\mathbf{v}\|_{\mathbf{H}^1(\Omega)}\|q\|_{L^2(\Omega)}}\geqslant\alpha>0 \tag{3}$$

### 2.1. Conforming finite element discretization for Stokes problem

We now discretize (2) by the finite element method by choosing finite dimensional spaces $\mathbf{V}_N\in\mathbf{H}_0^1(\Omega)$ and $M_N\in L_0^2(\Omega)$ of piecewise polynomials that approximate the velocity and pressure, respectively. Our problem can then be stated as: Find a discrete velocity $\mathbf{u}_N\in\mathbf{V}_N$ and a discrete pressure $p_N\in M_N$ such that, $\mu(\nabla\mathbf{u}_N,\nabla\mathbf{v}_N)-(\nabla\cdot\mathbf{v}_N,p_N)=(\mathbf{f},\mathbf{v}_N)$ and $(\nabla\cdot\mathbf{u}_N,q_N)=0$, for all $(\mathbf{v}_N,q_N)\in\mathbf{V}_N\times M_N$. Further, the discrete problem has a unique solution $(\mathbf{u}_N,p_N)\in(\mathbf{V}_N, M_N)$ if the following discrete *inf–sup* stability condition holds,

$$\inf_{q\in M_N}\sup_{\mathbf{v}\in\mathbf{V}_N}\frac{b(\mathbf{v},q)}{\|\mathbf{v}\|_{\mathbf{H}^1(\Omega)}\|q\|_{L^2(\Omega)}}\geqslant\alpha(N)>0 \tag{4}$$

### 2.2. Mortar hp finite element discretization for Stokes problem

We now partition the domain $\Omega$ into $S$ non-overlapping polygonal subdomains $\{\Omega_i\}_{i=1}^S$, which are geometrically conforming by which we mean that $\partial\Omega_i\cap\partial\Omega_j$ $(i<j)$ is either empty, a vertex, or a collection of entire edges of $\Omega_i$ and $\Omega_j$. In the latter case, we denote this interface as $\Gamma_{ij}$ $(i<j)$ and this will consist of individual common edges $\gamma,\gamma\subset\Gamma_{ij}$. (Let us point out that the analysis can be extended to the case of overlapping non-matching grids by following Cai *et al.* [18]). Let us define the interface set $\Gamma$ to be the union of the interface intersections $\partial\Omega_i\cap\partial\Omega_j$ $(i<j)$, which result in a non-empty $\Gamma_{ij}$. We further subdivide $\Omega_i$ into triangles and parallelograms by *regular* families of meshes $\{\mathcal{T}_h^i\}$. Let the maximum size of triangulation of subdomain $\Omega_i$ be $h_i$. Note that the triangulations over different $\Omega_i$ are independent of each other, with no compatibility enforced across interfaces. Let us stress that only the velocity space and not the pressure space will be subjected to any particular continuity constraints. For $K\subset\mathbb{R}^n$ and $k\geqslant 0$ integer, let $\mathcal{P}_k(K)$ denote the set of polynomials of total degree $\leqslant k$ on $K$ while $\mathcal{Q}_k(K)$ denotes the set of polynomials of degree $\leqslant k$ in each variable. Denote $\mathbf{Q}_k(K)=\mathcal{Q}_k(K)\times\mathcal{Q}_k(K)$. Let $\mathbf{k}$ be a degree vector, $\mathbf{k}=\{k_1,k_2,\ldots,k_S\}$ which specifies the degree used over each subdomain and denote $k=\min_{1\leqslant i\leqslant S}\{k_i\}$. Let us assume that the following local families of piecewise polynomial velocity and pressure spaces are given on $\Omega_i$,

$$\mathbf{V}_{h,k_i}^i=\{\mathbf{u}\in\mathbf{H}^1(\Omega_i)\,|\,\mathbf{u}|_K\in\mathbf{Q}_k(K)\ \text{for}\ K\in\mathcal{T}_h^i,\ \mathbf{u}=0\ \text{on}\ \partial\Omega_i\cap\partial\Omega\}$$

$$M_{h,k_i}^i=\{q\in L^2(\Omega_i)\,|\,q|_K\in\mathcal{P}_{k-1}(K)\}$$

 

Note that $\mathbf{Q}_k/\mathscr{P}_{k-1}$ has been shown to be uniformly divergence stable by Bernardi and Maday in Reference [19]. We now define a non-conforming space $\tilde{\mathbf{V}}_{h,\mathbf{k}}=\{\mathbf{u}\in\mathbf{L}^2(\Omega)\,|\,\mathbf{u}|_{\Omega_i}\in\mathbf{V}^i_{h,k_i}\}$. It can be noted that, $\tilde{\mathbf{V}}_{h,\mathbf{k}}\not\subset\mathbf{H}^1_0(\Omega)$ and hence cannot be used for finite element calculations.

Since the meshes $\mathscr{T}^i_h$ are not assumed to conform across interfaces, two separate trace meshes can be defined on $\Gamma_{ij}$, one from $\Omega_i$ and the other from $\Omega_j$. In addition to the meshes, the polynomial degrees may also be different across interfaces. Given $\mathbf{u}\in\tilde{\mathbf{V}}_{h,\mathbf{k}}$, we denote the traces of $\mathbf{u}$ on $\Gamma_{ij}$ from each of the domains $\Omega_i$ and $\Omega_j$ by $\mathbf{u}^i$ and $\mathbf{u}^j$, respectively. Then we can define the global non-conforming velocity space to be,

$$\mathbf{V}_{h,\mathbf{k}}=\left\{\mathbf{u}\in\tilde{\mathbf{V}}_{h,\mathbf{k}}\;\middle|\;\int_\gamma(\mathbf{u}^i-\mathbf{u}^j)\;\chi\,\mathrm{d}s=0\;\;\forall\;\chi\in\mathbf{S}^{\gamma,ij}_{h,\mathbf{k}}\;\;\forall\;\gamma\subset\Gamma_{ij}\subset\Gamma\right\} \tag{5}$$

where $\mathbf{S}^{\gamma,ij}_{h,\mathbf{k}}$ is a space of Lagrange multipliers for each edge $\gamma\subset\Gamma_{ij}$. (Note that $\mathbf{V}_{h,\mathbf{k}}\subset\tilde{\mathbf{V}}_{h,\mathbf{k}}$ and it enforces the inter-domain continuity in a *weak* sense). In the *mortar finite element method* (see References [1, 20, 5, 8] and the references therein) the Lagrange multiplier space $\mathbf{S}^{\gamma,ij}_{h,\mathbf{k}}$ is defined in the following way. Let the mesh $\mathscr{T}^i_h$ induce a mesh $\mathscr{T}^i_h(\Gamma_{ij})$ on $\Gamma_{ij}$. Let $\gamma\subset\Gamma_{ij}$ and denote the subintervals of this mesh on $\gamma$ by $I_l,\;0\leqslant l\leqslant N$. Let,

$$S^{\gamma,ij}_{h,\mathbf{k}}=\{\chi\in C(\gamma)\,|\,\chi|_{I_l}\in\mathscr{P}_{k_i}(I_l),\;\;l=1,\ldots,N-1,\;\;\chi|_{I_l}\in\mathscr{P}_{k_i-1}(I_l)\;\;l=0,N\} \tag{6}$$

Then we set, the Lagrange multiplier space to be $\mathbf{S}^{\gamma,ij}_{h,\mathbf{k}}=S^{\gamma,ij}_{h,\mathbf{k}}\times S^{\gamma,ij}_{h,\mathbf{k}}$. Note that imposing the mesh and degree on $S^{\gamma,ij}_{h,\mathbf{k}}$ from the domain $\Omega_i$ as has been done here is quite arbitrary, and these can be taken from the domain $\Omega_j$ as well, without changing the results obtained. Seshaiyer and Suri [7] recently provided other choices for the Lagrange multiplier space.

The global pressure space is given by, $M_{h,\mathbf{k}}=\{q\in L^2_0(\Omega)\,|\,q|_{\Omega_i}\in M^i_{h,k_i}\}$. This space is provided with the $L^2(\Omega)$-norm while the global velocity space is endowed with a discrete Hibertian broken norm, $\|\mathbf{u}\|^2_*=\sum_{i=1}^S\|\mathbf{u}\|^2_{\mathbf{H}^1(\Omega_i)}$. The mortar finite element discretization to (2) is then given as follows: Find $(\mathbf{u}_{h,\mathbf{k}},p_{h,\mathbf{k}})\in\mathbf{V}_{h,\mathbf{k}}\times M_{h,\mathbf{k}}$ satisfying,

$$a_S(\mathbf{u}_{h,\mathbf{k}},\mathbf{v})+b_S(\mathbf{v},p_{h,\mathbf{k}})=(\mathbf{f},\mathbf{v})\quad\text{and}\quad b_S(\mathbf{u}_{h,\mathbf{k}},q)=0 \tag{7}$$

where, $a_S(\mathbf{u},\mathbf{v})=\mu\sum_{i=1}^S(\nabla\mathbf{u},\nabla\mathbf{v})_{\Omega_i}$ and $b_S(\mathbf{v},q)=-\sum_{i=1}^S(\nabla\cdot\mathbf{v},q)_{\Omega_i}$. Further, problem (7) has a unique solution if the following discrete *inf–sup* condition holds (see Ben Belgacem *et al.* [13] for more details): There exists a constant $\alpha'$ such that,

$$\inf_{q_{h,\mathbf{k}}\in M_{h,\mathbf{k}}}\;\sup_{\mathbf{v}_{h,\mathbf{k}}\in\mathbf{V}_{h,\mathbf{k}}}\frac{b_S(\mathbf{v}_{h,\mathbf{k}},q_{h,\mathbf{k}})}{\|\mathbf{v}_{h,\mathbf{k}}\|_*\;\|q_{h,\mathbf{k}}\|_{L^2(\Omega)}}\geqslant\alpha'>0 \tag{8}$$

The precise choice for $\alpha'$ is derived in Reference [13] and is shown to be independent of the number of subdomains. We then have the following global convergence error estimate:

*Theorem 2.1*

Let the exact solution $(\mathbf{v},q)\in\mathbf{H}^1_0(\Omega)\times L^2_0(\Omega)$ satisfy $\mathbf{v}_i=\mathbf{v}|_{\Omega_i}\in\mathbf{H}^{l+1}(\Omega_i)$ and $q_i=q|_{\Omega_i}\in H^l(\Omega_i)$ for $i=1,\ldots,S$. Then for $v=\min(l,k_i)$ and $\alpha'$ given by (8) the discrete solution satisfies,

$$\|\mathbf{v}-\mathbf{v}_{h,\mathbf{k}}\|_*+\alpha'\;\|q-q_{h,\mathbf{k}}\|_{L^2(\Omega)}\leqslant C\sum_{i=1}^S\frac{h_i^v}{k_i^l}(|\log k_i|^{1/2}\|\mathbf{v}_i\|_{\mathbf{H}^{l+1}(\Omega_i)}+\alpha'\|q_i\|_{H^l(\Omega_i)}) \tag{9}$$

 

Note that although this estimate is *quasi-optimal* by the pollution term $\sqrt{|\log k_i|}$, it is very useful in practice for *hp* computations.

## 3. COMPUTATIONAL EXPERIMENTS

We now introduce an auxiliary unknown $\lambda_{h,\mathbf{k}}$, belonging to the Lagrange multiplier space $\mathbf{S}_{h,\mathbf{k}} = \mathbf{S}_{h,\mathbf{k}}(\Gamma) = \prod_{\Gamma_{ij}\subset\Gamma} \mathbf{S}_{h,\mathbf{k}}^{\gamma,ij}$. Defining the bilinear form $c_S(\mathbf{v},\chi) = \sum_{\gamma\subset\Gamma_{ij}\subset\Gamma} \int_\gamma (\mathbf{v}^i - \mathbf{v}^j)\chi\,\mathrm{d}s$ on $\tilde{\mathbf{V}}_{h,\mathbf{k}} \times \mathbf{S}_{h,\mathbf{k}}$, our problem becomes: Find $(\mathbf{u}_{h,\mathbf{k}}, p_{h,\mathbf{k}}, \lambda_{h,\mathbf{k}}) \in \mathbf{V}_{h,\mathbf{k}} \times M_{h,\mathbf{k}} \times \mathbf{S}_{h,\mathbf{k}}$ satisfying,

$$a_S(\mathbf{u}_{h,\mathbf{k}},\mathbf{v}) + b_S(\mathbf{v}, p_{h,\mathbf{k}}) + b_S(\mathbf{u}_{h,\mathbf{k}}, q) + c_S(\mathbf{v},\lambda_{h,\mathbf{k}}) + c_S(\mathbf{u}_{h,\mathbf{k}},\chi) = (\mathbf{f},\mathbf{v}) \tag{10}$$

We now report some computational experiments for the mortar mixed formulation (10) for stationary Newtonian flow on a L-Shaped domain $\Omega$, shown in Figure 1. This domain is subdivided into two rectangular subdomains $\Omega_1$ and $\Omega_2$ by the interface AO.

For our experiments, we let the viscosity $\mu = 1$ and consider an exact solution that satisfies, $\mathbf{u} = 0$ on the edges OC, OD and, $-\Delta\mathbf{u} + \nabla p = 0$. It is given by

$$\mathbf{u}(r,\theta) = r^\lambda[(1+\lambda)\sin(\theta)\Psi(\theta) + \cos(\theta)\Psi'(\theta),\ \sin(\theta)\Psi'(\theta) - (1+\lambda)\cos(\theta)\Psi(\theta)] \tag{11}$$

$$p(r,\theta) = \frac{-r^{\lambda-1}[(1+\lambda)^2\Psi'(\theta) + \Psi'''(\theta)]}{1-\lambda} \tag{12}$$

with,

$$\Psi(\theta) = \frac{\sin((1+\lambda)\theta)\cos(3\lambda\pi/2)}{(1+\lambda) - \cos((1+\lambda)\theta)} - \frac{\sin((1-\lambda)\theta)\cos(3\lambda\pi/2)}{(1-\lambda) + \cos((1-\lambda)\theta)} \quad \text{and} \quad \lambda = 0.54448$$

Note that this solution exhibits a corner singularity phenomena at the reentrant corner O. In our experiments, we consider *tensor product meshes*, where $\Omega_2$ is divided into $n^2$ rectangles

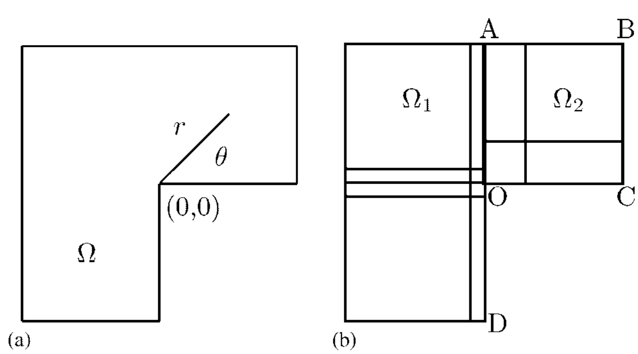


Figure 1. (a) L-shaped domain and (b) tensor product mesh for $m = n = 2$.

 

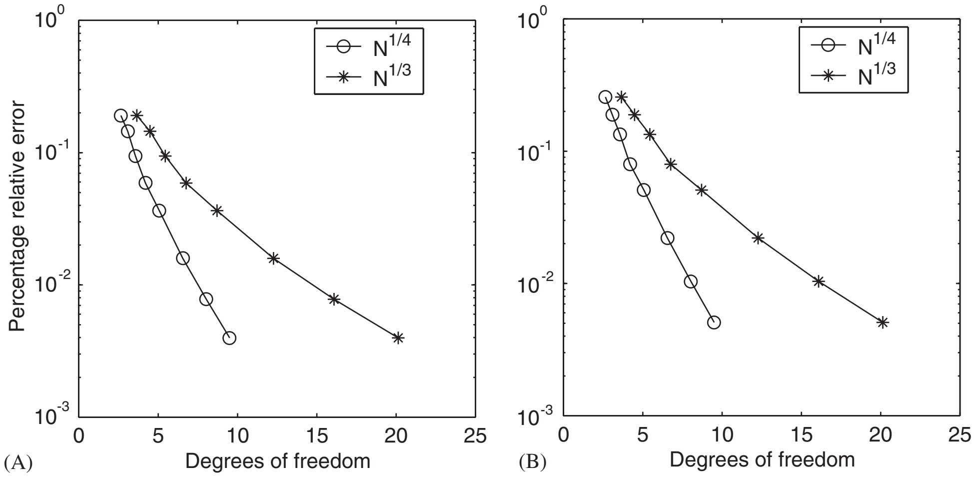


Figure 2. Exponential convergence for the mortar method over geometric meshes.

and $\Omega_1$ is divided into $2m^2$ rectangles (see Figure 1). Since the mesh on $\Omega_1$ is symmetric about $y=0$, in the sequel we only describe the mesh on the top half.

First, we consider *hp*-version of the non-conforming method on *geometric* meshes. We take $m=n$, and along the $x$ and $y$ axes, take the grid points, $x_0=0$, $x_j=\sigma_i^{n-j}$, $j=1,\ldots,n$, where $\sigma_i$ is the geometric ratio used on $\Omega_i$. The optimal value was provided by Gui and Babuška [21] to be 0.15, but we take $\sigma_1=0.17$ and $\sigma_2=0.13$ to make the method non-conforming. In Figure 2, we plot the log(relative error) vs $N^{1/4}$ (where $N$ is the number of degrees of freedom) which results in a straight line, showing that the *hp*-version gives $C\mathrm{e}^{-\nu N^{1/4}}$ convergence. The reason we only get an exponent of $N^{1/4}$ rather than $N^{1/3}$ is that our tensor product meshes have too many extra degrees of freedom compared to the optimized meshes that were presented by Guo and Babuška in Reference [2]. We have also plotted the error vs $N^{1/3}$ in Figure 2, for comparison. Panel (A) shows the results of velocity and panel (B) for the pressure.

Next, in Figure 3, we compare the conforming finite element methods ($\sigma_1=\sigma_2=0.13$ and 0.17) with the mortar method ($\sigma_1=0.17, \sigma_2=0.13$), using $n=4$ layers. We see the characteristic 'S' shaped convergence curve being clearly visible for both the velocity (Panel (A)) and pressure (Panel (B))—the middle part denoting the exponential *p*-version convergence phase, which at the end flattens out to an algebraic rate. The figure also indicates that the convergence rates obtained by employing the non-conforming method does not deteriorate. Note that the conforming method for 0.13 behaves better than 0.17 as $N$ increases, showing over-refinement is better than under-refinement.

We now show some results on computations for the error in the Lagrange multiplier which is chosen according to (6). Note that the non-smooth solution in (11) has a $r^\lambda$ singularity which implies that $\mathbf{u}\in\mathbf{H}^{\lambda+1-\varepsilon}(\Omega)$. Therefore, the gradient $\nabla\mathbf{u}\in\mathbf{H}^{\lambda-\varepsilon}(\Omega)$. Hence, the normal derivative (which corresponds to the Lagrange multiplier) on the interface $\gamma$ is given by $\partial\mathbf{u}/\partial n=\nabla\mathbf{u}\cdot n|_\gamma\in\mathbf{H}^{\lambda-1/2-\varepsilon}(\gamma)$. We consider the *h*-version using *uniform* meshes on $\Omega_1$ and $\Omega_2$. For this, we take $m$ grid points along both the $x$- and $y$-axis for $\Omega_1$ (top half) and $n$ for $\Omega_2$, and

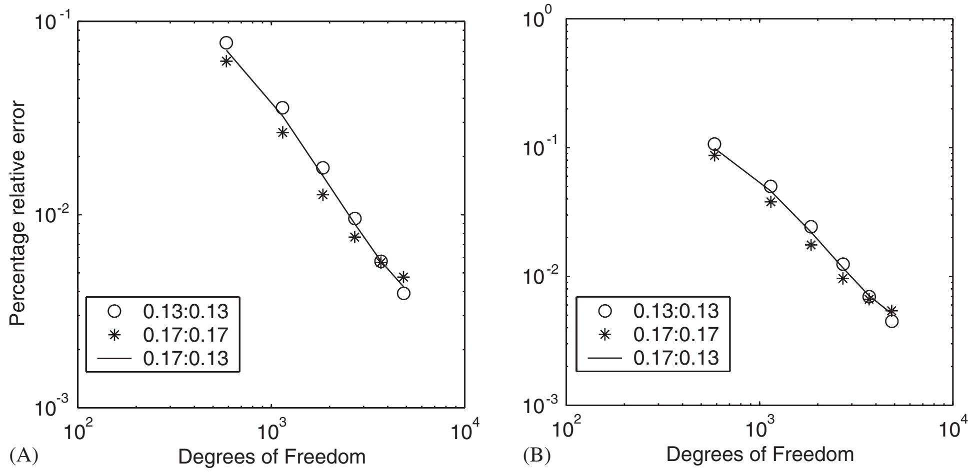


Figure 3. Comparison of mortar method with conforming FEM for $p$-version over geometric mesh.

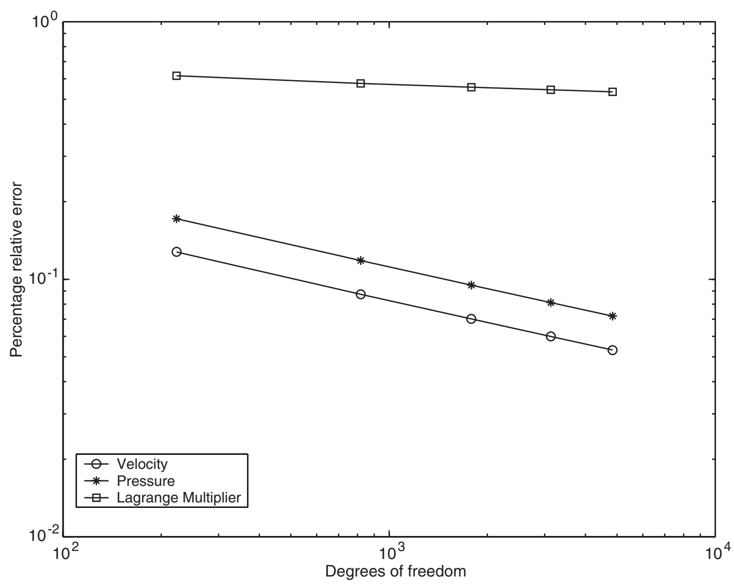


Figure 4. Error in velocity, pressure, Lagrange multiplier for $h$-version with uniform mesh.

use mixed mortar formulation (10) with the combinations $(m,n)\in\{(2,3),(4,6),\ldots,(10,15)\}$. The percentage relative error in the discrete $\mathbf{H}^1$-norm for the velocity, the $L^2$-norm for the pressure and the $\mathbf{L}^2$-norm for the Lagrange multipler are plotted in Figure 4. We observe a rate of $O(h^{\lambda})$ (where $\lambda = 0.54448$) for both the velocity and the pressure and a rate of $O(h^{\lambda-0.5})$ for the Lagrange multiplier as expected.

 

Next, we show the results of extracting point-wise derivatives along interface OA in Figure 1(b) using the non-conforming method, even when the singular solution in (11) and (12) is used. Since the derivatives of this unsmooth solution have a singular behaviour as $r \to 0$, we extract values at 19 equally spaced points in $[\frac{1}{20}, \frac{19}{20}]$. In Figure 5, we have plotted $u_x^1$ (the $x$-derivative of the first component of the velocity) as obtained from the exact solution, the average of the non-conforming solutions (from $\Omega_1$ and $\Omega_2$ using the mortar method), and the Lagrange multiplier $(-\lambda^1 = u_x^1)$ as obtained from the mortar method. The results are shown for the cases where the polynomial degree is $k=4$ and 8, respectively, when a geometric mesh with $n=2$, $\sigma_1 = 0.17$ and $\sigma_2 = 0.13$ is used. It is observed that the computed values are all comparable to the exact values. As expected, the Lagrange multiplier shows oscillations as $r \to 0$ for $k=4$ and the oscillations are minimized as the polynomial degree is increased to $k=8$. The results for $u_x^2$ (not shown) are similar. This suggests that stress extraction can be accurately performed even along interfaces when mortar methods are used in Stokes problems.

Finally, we consider the experiments where the non-conformity is due to the polynomial degree. In Figure 6, we show the percentage relative error in velocity for $h$ version over conforming uniform meshes on $\Omega_1$, $\Omega_2$ with $m=n=1,2,\ldots,8$ for the case of $(k_1,k_2)=\{(3,4),(3,3),(4,3),(4,4)\}$ where $k_i$ is the polynomial degree on $\Omega_i$, $i=1,2$. As expected, the overall error for the method with non-conforming polynomial degree behaves very similar to the method with conforming degrees in each domain. This suggests that using mortaring to selectively increase polynomial degrees can be very effective in treating parts of the domain where the solution is unsmooth (e.g. due to boundary layers or singularities).

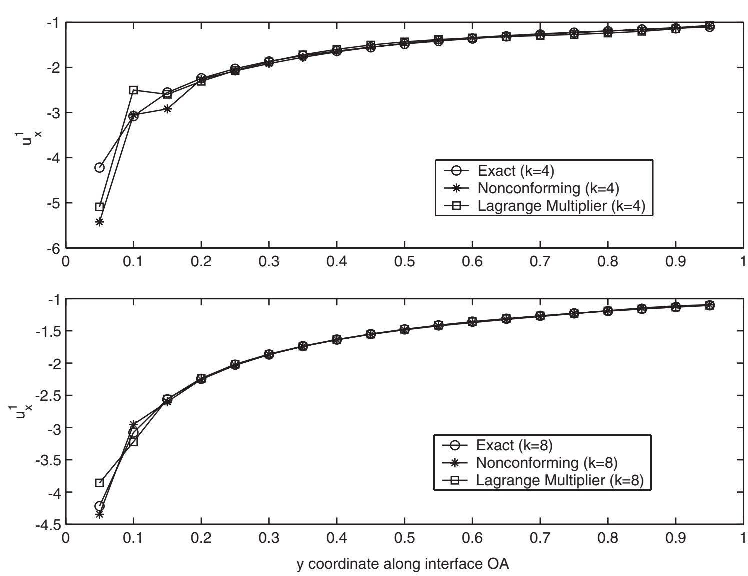


Figure 5. Point-wise extraction of $u_x^1$ along interface OA.

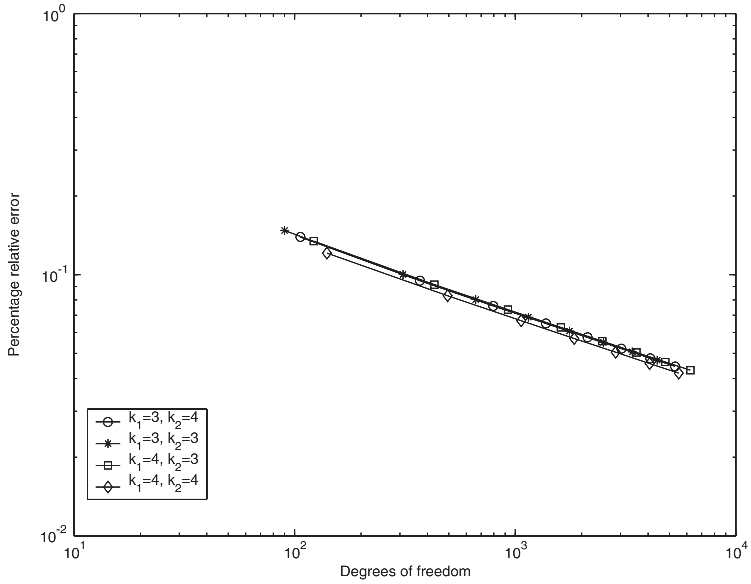


Figure 6. Error in velocity for *h* version for a conforming uniform mesh with different degrees on $\Omega_1$ and $\Omega_2$.


## ACKNOWLEDGEMENTS

This work was supported in part by the Air Force Office of Scientific Research, Air Force Research Laboratory, USAF under project order QAF185015203247 and by the National Science Foundation under grant DMS 0207327.


## REFERENCES


1. Bernardi C, Maday Y, Patera AT. Domain decomposition by the mortar element method. *Asymptotic and Numerical Methods for PDEs with Critical Parameters*, Kaper HG, Garbey M (eds). NATO Advanced Science Institutes Series C. Mathematical and Physical Science, vol. 384. Kluwer Academic Publication: Dordrecht, 1993, pp. 269–286.
2. Guo B, Babuška I. The *hp* version of the finite element method. *Computational Mechanics* 1986; **1**:21–41 (Part I), 203–220 (Part II).
3. Babuška I, Suri M. The *p* and *hp* versions of the Finite Element Method: Basic Principles and Properties. *SIAM Review* 1994; **36**:578–632.
4. Schwab C, Suri M. The *p* and *hp* versions of the finite element method for problems with boundary layers. *Mathematics of Computation* 1996; **65**:1403–1429.
5. Seshaiyer P, Suri M. Uniform *hp* convergence results for the mortar finite element method. *Mathematics of Computation* 2000; **69**:521–546.
6. Seshaiyer P, Suri M. Convergence results for non-conforming *hp* methods: The mortar finite element method. *Contemporary Mathematics* 1998; **218**:467–473.
7. Seshaiyer P, Suri M. *hp* submeshing via non-conforming finite element methods. *Computer Methods in Applied Mechanics and Engineering* 2000; **189**:1011–1030.
8. Ben Belgacem F, Seshaiyer P, Suri M. Optimal convergence rates of *hp* mortar finite element methods for second-order elliptic problems. *RAIRO Mathematical Modelling and Numerical Analysis* 2000; **34**:591–608.
9. Seshaiyer P. Stability and convergence of non-conforming *hp* finite element methods. *Computers and Mathematics with Applications* 2002; at press.
10. Ben Belgacem F. The mixed mortar finite element method for the incompressible Stokes equations: Convergence Analysis. *SIAM Journal on Numerical Analysis* 2000; **37**:1085–1100.


 

11. Achdou Y, Abdoulaev G, Hontand JC, Kuznetsov YA, Pironneau O, Prud'homme C. Nonmatching grids for fluids. *Contemporaty Mathematics* 1998; **218**:3–22.
12. Ben Belgacem F, Bernardi C, Chofri N, Maday Y. Inf-sup condition for the mortar spectral element discretization for the Stokes problem. *Numerische Mathematik* 2000; **85**:257–281.
13. Ben Belgacem F, Chilton LK, Seshaiyer P. The *hp* mortar finite element method for the mixed elasticity and stokes problems. *Computers and Mathematics with Applications* 2002; at press.
14. Baaijens FPT. A fictitious domain/mortar element method for fluid-structure interaction. *International Journal for Numerical Methods in Fluids* 2001; **35**(7):743–761.
15. Levin GL, Iskandarani M, Haidvogel DB. A nonconforming spectral element ocean model. *International Journal for Numerical Methods in Fluids* 2000; **34**(6):495–525.
16. Rønquist EM. Convection treatment using spectral elements of different order. *International Journal for Numerical Methods in Fluids* 1996; **22**(4):241–264.
17. Brezzi F, Fortin M. *Mixed and Hybrid Finite Element Methods*, Springer Series in Computational Mathematics, vol. 15. Springer: New York, 1991.
18. Cai XC, Dryja M, Sarkis M. Overlapping non-matching grid mortar element methods for elliptic problems. *SIAM Journal on Numerical Analysis* 1999; **36**:581–606.
19. Bernardi C, Maday Y. Uniform inf-sup conditions for the spectral discretization of the Stokes problem. *Mathematical Models and Methods in Applied Sciences* 1999; **9**:395–414.
20. Ben Belgacem F. The mortar finite element method with Lagrange Multipliers. *Numerische Mathematik* 1999; **84**:173–197.
21. Gui W, Babuška I. The *hp* version of the finite element method in one dimension. *Numerische Mathematik* 1986; **3**:577–657.

 